An Acad Bras Cienc (2024) 96(Suppl. 1): e20230487 DOI 10.1590/0001-3765202420230487
Anais da Academia Brasileira de Ciências | *Annals of the Brazilian Academy of Sciences*
Printed ISSN 0001-3765 I Online ISSN 1678-2690
www.scielo.br/aabc | www.fb.com/aabcjournal

ENGINEERING SCIENCES

Mitigating interferences on LEO satellite downlinks of Earth exploration services by cognitive radio, adaptive modulation and coding techniques

RODOLFO ANTONIO DA SILVA ARAUJO, LUCIANO B.C. DA SILVA,
WALTER ABRAHÃO DOS SANTOS & MARCELO L. DE OLIVEIRA E SOUZA

Abstract: Upcoming Earth Exploration Satellite Services (EESS) missions, especially to monitor Brazilian diversified biomes, will require progressively higher data rates for downlink transmissions, besides the ability to share its frequency spectrum with cellular base stations. Both impact issues on spectral efficiency (in bps/Hz) and coexistence in frequency, time, location, etc. This paper proposes a technique suitable for LEO Earth Observation Satellites (EOS) by combining two strategies. We initially present the Cognitive Radio (CR) spectrum awareness and exploitation approaches to propose techniques for improving their uses. Next, we detail the Adaptive MODulation and CODing (MODCOD) techniques (ACM) based on DVB-S2X systems to increase RF power and spectral efficiencies. Finally, we evaluate our solution by monitoring the Signal to Interference plus Noise Ratio (SINR) and combining CR/MODCOD techniques. Two case studies are presented that demonstrate the proposed approach on Brazilian satellites developed by the National Institute for Space Research (INPE). A real in-situ characterization of the interfering scenarios was performed during the passes of the two EESS satellites that proves the effectiveness of spectral efficiency and coexistence.

Key words: Cognitive radio, Earth Exploration Satellite Services, high throughput satellites, modulation and coding, spectrum efficiency, spectral coexistence.

INTRODUCTION

Efforts should be engaged toward the future of the Earth Exploration Satellite Services (EESS) missions, especially in Brazil, to monitor the Brazilian territory's diversified agriculture and biomes, including the deforestation of the Amazon rainforest (AEB 2022). They aim to deploy small and medium-sized satellites with payloads employing ultra-high-resolution optical sensors or Synthetic Aperture Radars (SARs) that generate and require higher data rates for downlink transmissions.

Our ongoing thesis centralizes on identifying and mitigating the harmful effects on remote sensing digital data transmitted by Earth Observation Satellites (EOS) caused by interfering signals from fixed service radio links arriving in ground receiving stations. Fixed Service (FS) systems are Limited Private Services regulated by ANATEL (2013).

The plan is to manipulate the downlink transmission parameters in the Earth observation communication system (onboard TX and ground station RX), selecting them from part of Cognitive

Radio (CR) techniques in the underlay paradigm, to remove the imaging degradation caused by these interferences.

The whole concept of CR was first proposed and detailed by Joseph Mitola III in his PhD manuscript (Mitola III 2000). In recent times, in ETSI (2016), the CR System (CRS) is defined as:

CRS employs technology that allows the system to obtain a knowledge of its operational and geographical environment, established policies and its internal state, to adjust its operational parameters and protocols dynamically and autonomously according to the knowledge acquired to achieve predefined objectives.

We will consider the Cognitive Radio (CR) concept as a potential proposition to address the spectrum scarcity obstacle in the development of shared satellite-terrestrial wireless networks. Since its conception, groups of researchers, academic institutions, industries, and regulatory and standardization bodies have made significant efforts to materialize the CR concept. Despite this, practical issues must be considered since the strategy requires adapting the transmitter system based on the surrounding radio environment (Sharma et al. 2015).

Impairments, such as noise uncertainty, channel and interference indeterminacy, transceiver hardware imperfections, signal uncertainty, and synchronization problems, may affect a practical CR system's performance. For this reason, investigating realistic solutions in a real satellite use case to overcome different impairments is highly valuable for implementing the cognitive concept.

This article initially provides the surveyed techniques that enable CR communications with interferences in the underlay paradigm; then, we develop and adapt/implement the existing approaches to address these interferences.

Breakthrough spectral exploitation methods for high throughput communication satellites combined with architectures from the CR paradigm are the most promising solution to achieve the required high data rate and spectrum sharing (Garhwal & Bhattacharya 2012) goals in the coming years.

In this sense, we highlight the essential aspects of CR spectral awareness and exploitation to create a basis for spectrum efficiency improvement techniques for EESS (Sharma et al. 2013): to increase the satellite data throughput, even with mitigating the occurrence of interference in this service. Based on that, we propose a novel combination of the Cognitive Radio (CR) approach and Adaptive MODulation and CODing (MODCOD) technique (ACM) to mitigate interferences in the downlink of Earth exploration services on Low Earth Orbit (LEO) satellites for spatial, temporal, and spectral coexistence while achieving the goal of high throughput. The MODCOD techniques are based on the intelligent application of high-efficient and improved (to non-linearities) modulation, combined with efficient channel coding, i.e., error correction codes (ETSI 2020).

Scarcity has motivated the progression of the CR communication concept (Mitola III 2000), which comprises a variety of techniques enabling spectral coexistence. In this context, our ongoing thesis should provide a technical solution for CR on the underlay paradigm that has the function of becoming a tool to solve interference failures resulting from the coexistence of Primary Users (LU/PU) and unlicensed Cognitive/Secondary Users (CU/SU) over the same frequency band.

Satellite communication CR approaches have only recently gained significant effort in the literature. In terrestrial and satellite contexts, there are two widely used approaches for enhancing the spectral efficiency of current wireless systems (Sharma et al. 2015): i) Dynamic Spectrum Access (DSA)

(in interweave paradigm), by using opportunistic spectrum access; and ii) Spectrum Sharing (SS) (in underlay), by allowing the sharing of the available spectrum between primary and secondary systems.

The concept of CR communication has been widely proposed to solve the spectrum scarcity dilemma, comprising a variety of approaches and techniques to allow coexistence in the same spectral band between primary and secondary users.

In the EOS downlink scheme, we can improve the functional performance of onboard high data rate transmitters to fulfill the requirements of bandwidth and use of RF power efficiently, employing MODCOD techniques in an ACM (Adaptive Coding and Modulation) system (Colin et al. 2016, CCSDS 2013).

There will be cases where simultaneous transmissions from primary and secondary users in the same spectral band at the same time and location will be required, for example, as described in Wang et al. (2018): GEO satellites as SUs with LEO satellites as PUs.

Therefore, the Cognitive Radio communication approach has been revealing solutions to overcome the spectrum scarcity in current wireless systems as well as applications that provide spectral coexistence of users. CR has promising solutions: 1) to reconcile the conflicts between the growing demand for spectrum and its underutilization; and 2) to increase the overall efficiency of spectrum exploitation.

The applicability of the CR techniques that are available to allow the spectral coexistence of PUs and SUs is only possible with the advanced algorithmic functions characteristic of Software Defined Radios (SDRs) (Ibrahim & Galal 2016).

We organize this article as follows. The next section presents the **materials and methods** used in CR paradigm exploitation techniques, introduces the MODCOD in ACM technologies, and also describes the coexistence/interfering scenario of the EESS downlink hinting at our combining solution as the technique used to mitigate the harmful effects caused by the interferences in the desired signal; **results** section presents the main analytical solutions for the signal to interference plus noise ratio and their results in the downlink given by the application of the chosen combined MODCOD/CR strategy in case studies – the WFI interfering communication system. In the last sections we discuss the results of case studies and concludes this paper.

MATERIALS AND METHODS

This section presents a concise review of CR spectrum exploitation techniques and the interfering scenario calculating the link budget with the real parameters considering the satellite downlink; subsequentially, we introduce the combination of MODCOD in ACM mode plus CR strategy chosen to mitigate the interfering harmful effects on imagery data and implemented the technique.

Cognitive Radio paradigms & techniques

We can describe the operational techniques available in all the proposed CR systems as continuous cognitive cycles (Sharma et al. 2015) in the following sequence as shown in Figure 1:

1. *Spectrum Awareness (Sensor)*: the first task for a CR is to be aware of its surrounding radio environment,

2. *Analysis and Decision (Controller)*: to analyze the information obtained and take an intelligent decision on how to use the available resources effectively, and

3. *Spectrum Exploitation (Adaptation) (Actuator)*: i.e., the CR autonomously adapts its operational parameters such as transmit power, operating frequency, modulation and coding schemes, antenna pattern bean or polarization, etc. to any environmental conditions to exploit the available spectral opportunities effectively.

In this sense, the spectrum awareness capability enables a CR to gain information about the spectral opportunities dynamically while the spectrum exploitation capability assists the CR to exploit the available spectral opportunities efficiently.

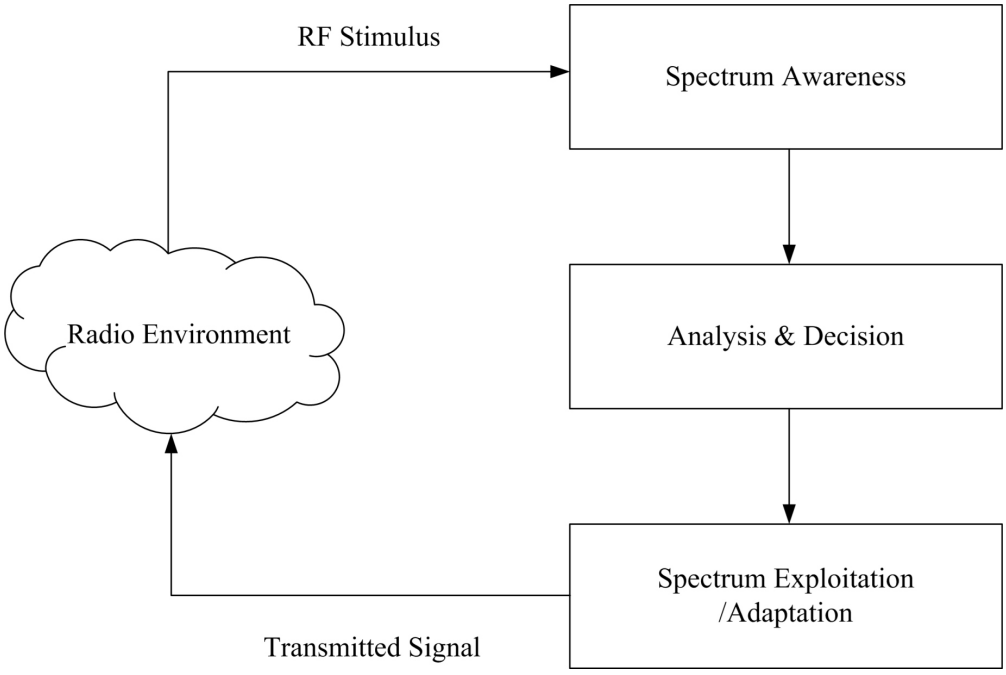

Figure 1. A simplified cognitive cycle.

Spectrum exploitation techniques

Based on the knowledge level of the PU transmission signals, the existing spectrum exploration techniques can be classified into the interweave, underlay, and overlay paradigms (Sharma et al. 2015). Figure 2 illustrates the representation of the signals for the exploitation techniques. According to Sharma (2014), we may define:

1. Interweave: this spectral coexistence approach incorporates opportunistic or interference avoidance techniques that aim to allow cognitive radios to communicate opportunistically by using spectral holes (Fig. 2a) either in space, time, and frequency that are not occupied by PUs. Therefore, no interference occurs in the ideal case. CR must constantly identify and monitor the surrounding environment to predict the underutilization of each fraction of the spectrum for SUs

to access until the primary activity remains idle. Polarization and angular dimensions may also be additional dimensions for spectrum exploitation purposes in interweave communication.

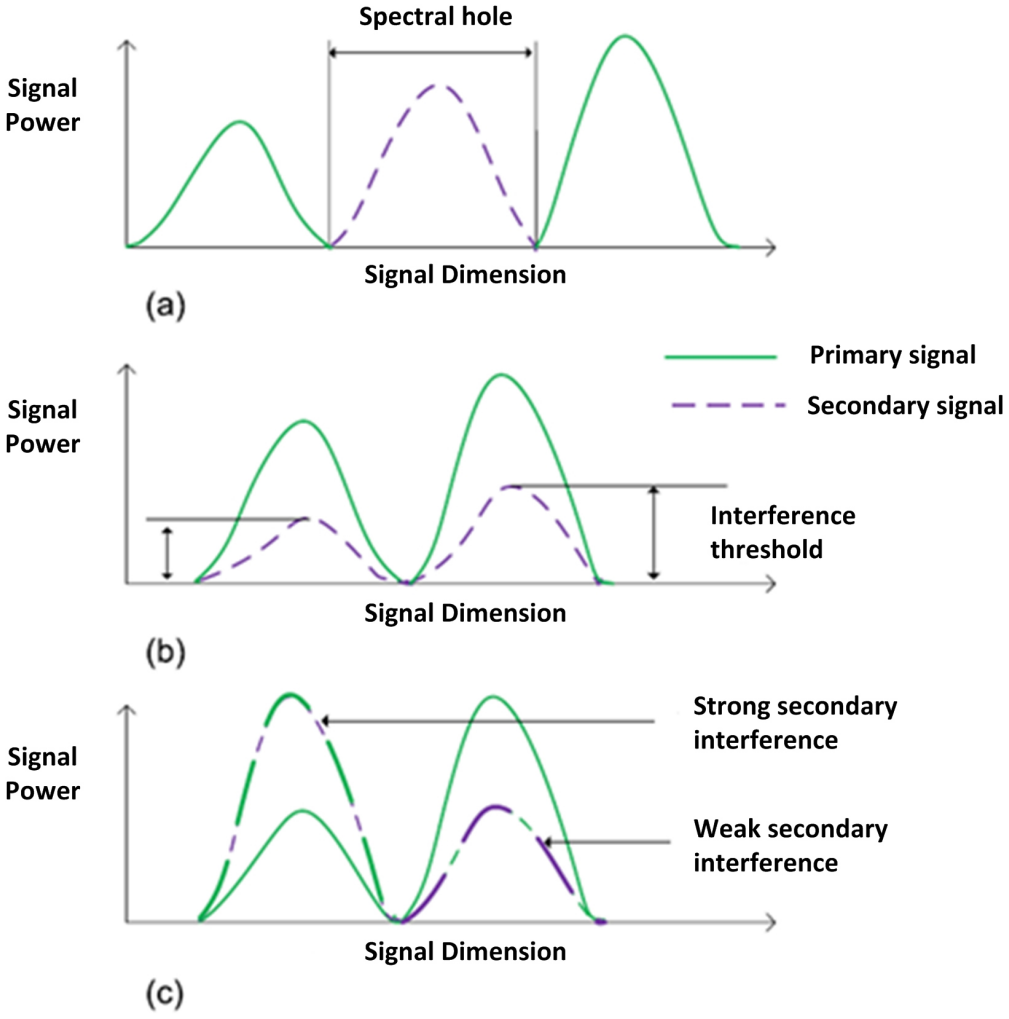

Figure 2. Representation of interweave (a), underlay (b), and overlay (c) techniques (Sharma et al. 2015).

2. Underlay: in this paradigm, simultaneous cognitive and non-cognitive transmissions are allowed in the same frequency band as long as the interference level on the PU side remains acceptable at the threshold-defined level (Fig. 2b). The maximum allowable interference level on the PU can be modeled by the interference temperature concept (Bousquet & Maral 2009) and is regulated by any local federal policy (FCC Spectrum Policy Task Force in Federal Communications Commission et al. (2003), for example). PU system information such as SNR, channel parameters, and DoAs (direction of arrivals) are required to perform the underlay techniques. Besides, underlay communication can be implemented by using one or a combination of the following methods: (i) beamforming with the use of multiple antennas or phased array, (ii) dynamic resource allocation (carrier and power) in the secondary transmitter (ST), (iii) spread spectrum approaches by spreading the secondary signal below the primary signal noise floor and then dispreading at the secondary receiver (SR), (iv) by using Exclusion Zone (EZ) principle.

3. Overlay: networks based on this paradigm are characterized by interference mitigation using advanced encoding and transmission strategies in the ST, as well as when the SU transmits simultaneously with the PU (Fig. 2c). In short, the interference caused by the ST to the PR can be compensated using a part of the power of the SU to retransmit the PU message (da Silva et al. 2020). In this paradigm, PU shares information about its signal codebooks and messages with SU. Cognitive devices can therefore enhance and assist primary transmission rather than compete for spectrum access. More precisely, SU listens to the messages sent by the PU sources and uses these messages to eliminate the interference generated by the primary communication on the SR side or to improve the performance of the primary transmission by retransmitting the accumulated messages to the PR. This last case allows the ST to transmit both signals simultaneously if the total transmission power is sufficient to cover the energy needed for its communication and retransmission operation. Overlay techniques are the most suitable techniques for integrated systems where there is a high degree of cooperation between the terrestrial and satellite networks. In practice, this paradigm is difficult to implement due to the high level of cognition required between the primary and secondary systems. The ways to acquire the characteristics of the PU wave signal are using estimation approaches, such as MODCOD classification and detection, estimation of cyclic frequencies, pilot, and frame header, etc.

ACM technique based on DVB-S2X

By continuing our presentation of the evolved technical concepts, we emphasize that the ACM technique itself does not represent a direct Cognitive Radio approach. However, this technique, when combined with a CR approach, benefits satellite cognitive applications. Then, we will introduce its concepts and show how this method can be implemented to obtain better bandwidth and RF power efficiencies and its application to solve the interference effect in the EOS data downlink–image degradation.

Well-recognized techniques for high data rate (HDR) are based on the proper use of modulation and coding. As an example, Low Density Parity Check (LDPC) encoding followed by Amplitude-Phase Shift Keying (APSK) modulation will be the next generation standard for HDR downlink data (Addabbo et al. 2014) under the DVB-S2X standard (CCSDS 2021). The basic idea of LDPC codes is to use a simple implemented encoder that can produce long codewords with exceptional word spacing properties and low-complexity techniques based on the encoder's predefined structure.

Moreover, APSK constellation performs better than the usual MPSK for having a greater distance between constellation points or than QAM in the presence of nonlinear distortions caused by power amplifier (TWTA or SSPA) operating in the saturation.

The system's parameter to be controlled can be summarized as i) code performance at the defined Bit Error Rate (BER). For LDPC codes, there is a region after which performance stabilizes. This region is called the error floor, and the operating point must be located rationally far from the error floor; ii) the code rate selection gives the expected performance; iii) encoding and decoding complexity.

DVB-S2X is the second-generation extensions standard for Digital Video Broadcasting (CCSDS 2021). This modulation-coding format for high data rate telemetry is based on LDPC codes combined

with eight selected modulation formats (QPSK, 8PSK, 8APSK, 16APSK, 32APSK, 64 APSK, 128 APSK, and 256 APSK) and with a wide range of code rates (1/4 to 9/10), ranging in spectral efficiency from 0.49 bit/s/Hz to 5.84 bit/s/Hz. The error correction is based on the concatenation of the BCH (Bose-Chaudhuri-Hocquenghem) code with the LDPC inner code. The coded block has a length of 64800 bits (normal frame) or 16200 bits (short frame). CCSDS recommendations limit the block length to 16200 bits for reducing the onboard memory and facilitating the iterative decoding at the earth stations.

Thus, in the satellite context, the on-board computer receives the telecommand to change the ACM mode parameters (MODCOD) from the Control and Tracking Center through a continuous feedback link; the Earth station reception system, ERG, carries out the real-time detection and monitoring E_b/N_0 (or $E_b/(I_0+N_0)$) [energy per bit to noise power spectral density ratio or to N_0 plus I_0 (interference power spectral density)] information which will make the on-board radio transmitter itself perform the necessary adaptations.

EESS downlink interfering scenario

Once we have briefly introduced the main techniques in the last sections, we investigate the performance of a satellite downlink in the presence of interfering signals plus noise (i.e., coexistence scenario). The main objective focuses on the communication system for receiving Earth observation images in the presence of interferences, by analyzing and mitigating its harmful effects.

The X band is the main frequency band (8.025–8.400 GHz) regulated for satellite-to-ground data transmission applications in EESS (ITU-R 2016). However, in the same frequency band, there are links of transmissions from fixed service radio stations (FS).

In this way, when considering the FS/EESS links coexistence scenario, the earth station may receive harmful interference from FS stations, operating with maximum EIRP and beamwidth that interfere at specific angles of azimuth and elevation on the satellite-receiving antenna.

On the other sense, we assume that the EESS downlink does not interfere with the FS system due to lower equivalent power flux density arriving at the FS antenna; Figure 3 shows the interference scenario with the satellite receiver system.

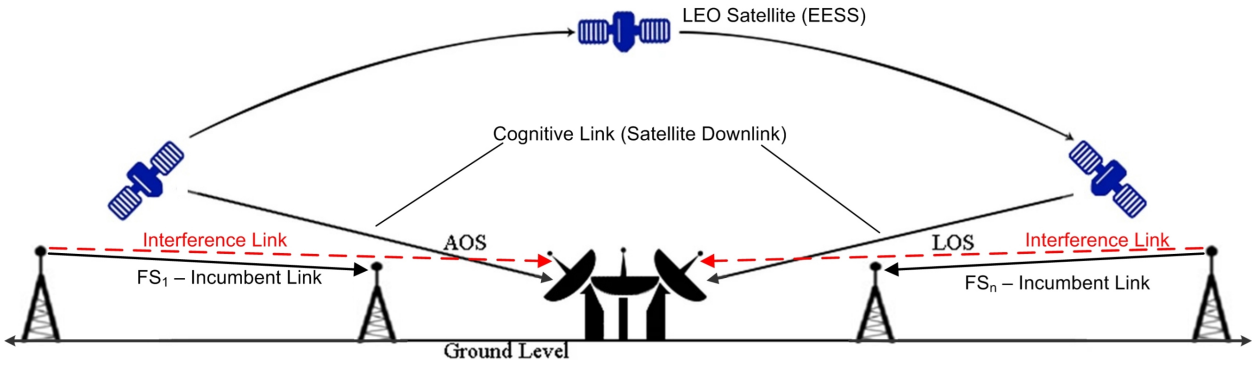

Figure 3. LEO satellite downlink scenario.

Specifications and recommendations concerning the evaluation of the EESS downlink system can be extracted from the International Telecommunication Union (ITU 1997) Report, which specifies

parameters for its implementation in the 8025 MHz - 8400 MHz band and the emission limit must not exceed the values according to Table I. Complementary recommendations are found in a Standard of CCSDS (2014).

Earth observation satellites respect these values by operating in the 375 MHz band (8025 and 8400 MHz) and as the power flux density on Earth is comparably low, this service does not interfere with FS links.

Table I. EESS emission limit recommended by ITU.

Frequency band MHz	Service	Limit in dB(W/m^2) for angle of arrival (δ) above the horizontal plane			Reference Bandwidth
8025-8500	Earth Exploration	0 - 5°	5° - 25°	25° - 90°	4 kHz
	Satellite	-150	-150+.5(δ-5)	-140	

Concerning our practical use case, which will be further discussed in the upcoming subsections, we point out that Brazil's main Earth observation satellite ERG is in the Cuiabá city-state of Mato Grosso (MT), at coordinates 17.7° latitude south and 56.0° longitude west. The region of Cuiabá and its surroundings is considered as the ideal location in Brazil for the installation of tracking antennas for remote sensing satellites in polar orbit. Positioned in the geodetic center of South America, this region provides a visibility radius of approximately 3000 km for only one tracking antenna for satellites with an altitude of around 750 km (INPE 2021).

Based on the above, this ERG allows the sending and receiving of data in real-time with coverage of the entire national territory and a large part of South America, avoiding the installation of more antennas to serve the satellite passages from one pole to the other.

When planned and implemented in the early 1970s, the first ERG was located on a site far from the Cuiabá urban area. With the expansion of the region, today INPE is next to the new Administrative Center of the capital of MT State, where there was a need to establish advanced telecommunications resources and, consequently, FS microwave links of Limited Private Services.

On this station, we will explore why the daily passages of the LEO satellite in certain orbits, with variable azimuths and elevations in the ERG, suffer from interference (links from Limited Private Services operators can degrade satellite reception).

The Earth-observation satellite CBERS-4 (China-Brazil Earth Resources Satellite-4), which was launched in 2014, consists of four cameras: PAN5/10, IRS, MUX, and WFI. The main purpose of Wide Field Imager (WFI), with a resolution of 64 m and 866 km of the swath, is to monitor the Amazon rainforest. Figure 4 shows a frame (set of scenes) from the CBERS-4 WFI image catalog covering twenty-six consecutive days. To examine how interference disturbs the WFI satellite images, we observe how the INPE image catalog is affected. In Figure 4, we can see that the ideal image frame forms an almost perfect circle outline.

But in Figure 5, we can observe the harmful effects on the set of images with the lack of points (coverage) in certain localizations of Brazil or South America, regions in azimuths to the northwest.

This is a fact due to the existence of an FS link in this geographic angular region. In the next Section, we discuss the real interfering scenario with more details, presenting the results.

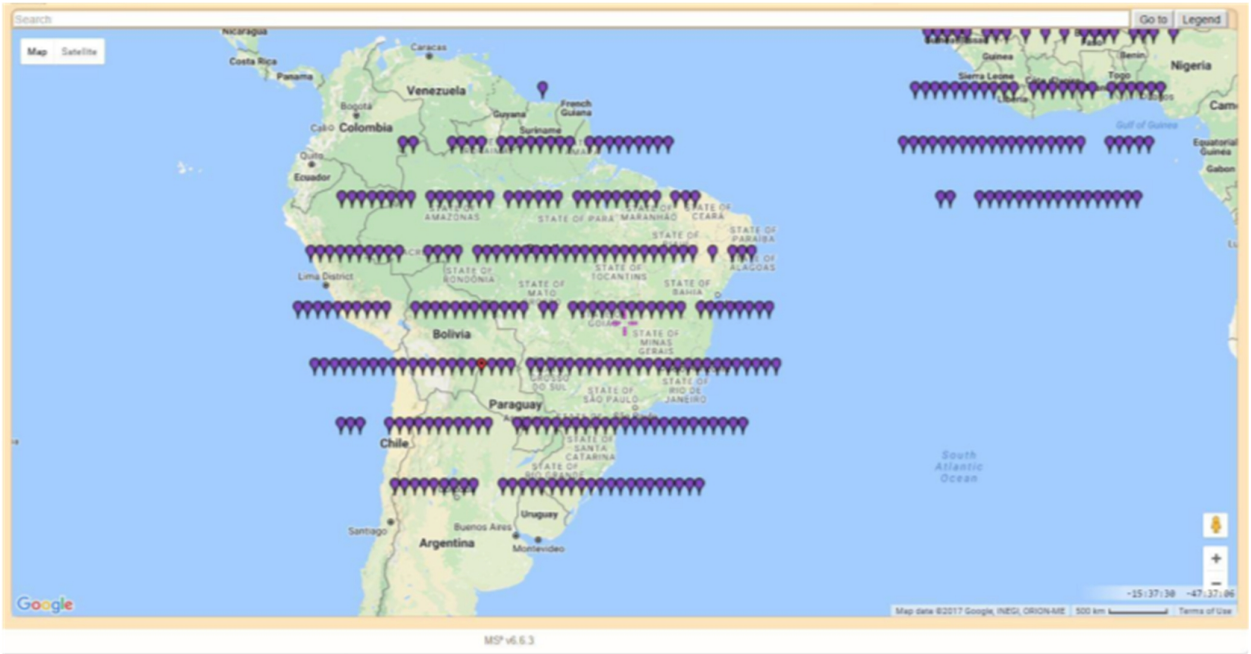

Figure 4. Depiction of a complete set of images from the CBERS-4 WFI camera over 26 days (INPE's Catalog). Source: (DGI-INPE 2018).

Figure 5. Depiction of a partial set of images (due to failures) of the WFI camera over 26 days (INPE's Catalog). Source: (DGI-INPE 2018).

In addition, in Figures 4 and 5, we observe the images in passages across South America and Africa, resulting from the imaging and transmission received by the Cuiabá ERG in real-time (on daytime passages). Night passages conduct playback of recordings from the African territories, monitoring their important biomes in countries with bilateral agreements with Brazil for free image distribution.

As previously exposed, the interfering signal comes from FS links operating in the X-band frequency range. We verify by on-site measurements and calculations that the harmful interference does not occur in all satellite passes when in sight of the receiving station, but especially on elevations and azimuths crossing the FS signal beam.

Afterward, we will calculate the parameters of the interference link budget and use an example of the WFI camera transmission parameters.

Link budget calculations

The Earth observation satellite downlink parameter calculations, based on Bousquet & Maral (2009), are necessary to check the received interfering signal influences at satellite data receiving stations. Therefore, the intention is to quantify the harming effect on the signal to interference plus noise ratio (SINR) compared to the initial signal to noise ratio (SNR).

1. Signal to noise ratio parameters of link budget on the Earth observation satellite downlink with and without interference:

The carrier signal level at the front-end input of the Earth station receiver is given by:

$$C = P_s + G_{st} + G_{er} - L_{fs} - L_{oth}\ (dBW)$$

Where:

C is the carrier power in dBW;
P_s is the TX output power in dBW;
G_{st} is the transmitting antenna gain of the satellite in dB;
G_{er} is the receiving antenna gain of the Earth station in dB;
L_{fs} is the downlink free space loss in dB;
L_{oth} is the other losses in dB.
And:

$$(EIRP)_s = P_s + G_{st}\ (dBW)$$

$$L_{TOTAL} = L_{fs} + L_{oth}\ (dB)$$

Where:

$(EIRP)_s$ is the satellite Effective Isotropic Radiated Power, and
L_{TOTAL} is the total loss.

The ratio between the received signal carrier power (C) and the noise power spectral density (N_0), designated C/N_0 ratio in dBW-Hz, assesses the link performance. We can use other derived relations for performance verification, such as E_b/N_0 for digitally modulated carriers used in high information rate transmission. Thus,

$$\left(\frac{C}{N_0}\right)_{downl} = (EIRP)_s + \left(\frac{G}{T}\right)_e - L_{TOTAL} - k\ (dBWHz)$$

Where $\left(\frac{C}{N_0}\right)_{dl}$ is the downlink C/N_0,

$\left(\frac{G}{T}\right)_e$ is the figure of merit regarding the antenna gain to the noise temperature of Earth station receiver, and

k is the Boltzmann constant, which is considered as $-$ 228.6 dB (W/K/Hz).

The Signal to Noise Ratio for digital modulated carriers follows:

$$\frac{E_b}{N_0} = \frac{C}{N} \bullet \frac{BW}{R_b}\ ,\ where\ N = N_0 \times BW$$

or

$$\frac{E_b}{N_0} = \frac{C}{N_0} - 10\log_{10}(R_b) \quad (dB)$$

Where R_b is the transmitted bit rate at the required E_b/N_0 $[(E_b/N_0)_{req}]$ for the transmission system, which depends on the modulation scheme that will be employed and the BER for the specific application. Considering a downlink margin M of at least 3 dB (recommended by Wertz et al. 2011), we have the expression for the minimum value required:

$$\left(\frac{E_b}{N_0}\right)_{min,\ req} = (EIRP)_{min} + \left(\frac{G}{T}\right)_e - L_{TOTAL} - 10\log_{10}(R_b)\ - 3 + 228.6\ \ (dB)$$

Where the $(EIRP)_{min}$ is the minimum power required from the satellite transmitter to fulfill the specified M of the link budget and $(E_b/N_0)_{min,\ req}$ is the minimum signal to noise ratio required.

In the last equation, we can verify that the term L_{TOTAL} refers to the sum of free space loss and all other losses to be considered in the link budget, including atmospheric loss (gases, free atoms, and water vapor of terrestrial atmosphere), rain attenuation, polarization loss (mismatch between receiving antenna polarization and received wave) and transmitting - receiving antennas disappointment.

Losses between the TX power amplifier and the antenna shall get embedded in the EIRP calculation, and the losses between the receiving antenna and the receiver front-end (ohmic losses, receiver equivalent temperature, and antenna noise temperature) are considered in the Earth station G/T figure of merit. Finally, we need to consider the demodulation implementation loss provided by receiver/demodulator manufacturer.

Calculation with interference

It will be necessary to calculate and update the parameter employed in wireless communication systems with interference signals to give upper bounds on information throughput. This quantity is the Signal to Interference plus Noise Ratio (SINR), defined as the power of the signal of interest divided by the total interference power plus the noise power spectral density.

For digital communication, the interest is to get the ratio between the energy per bit by the sum of the interference power density and noise power spectral density, given by:

$$\left(\frac{E_b}{N_0 + I_0}\right)_{min,\ req}\ ,\ req : required$$

How,

$$\frac{C}{N} = \frac{E_b}{N_0} \bullet \frac{R_b}{BW}$$

then $\frac{C}{I} = \frac{E_b}{I_0} \bullet \frac{R_b}{BW_I}$

Where BW_I is the interference signal bandwidth.

$$\therefore \frac{E_b}{I_0} = \frac{C}{I} - 10\log_{10}\left(\frac{R_b}{BW_I}\right) \ (dB)$$

In reception with a matched filter, we assumed that the bandwidth of the symbol rate (R_s) limits the receiver bandwidth, BW_{Rs}.

$$\text{so,} \quad BW_I \equiv BW_{Rs}$$

Where R_S is the symbol rate. The E_b/I_0 is given by:

$$\frac{E_b}{I_0} = \frac{C}{I} - 10\log_{10}\left(\frac{R_b}{BW_{Rs}}\right) \ (dB)$$

Calculation of SINR: $((E_b/(N_0+I_0))_{total}$:

$$\left(\frac{E_b}{N_0}\right)_{downl} = a, \quad and \quad \frac{E_b}{I_0} = b$$

$$\therefore \left(\frac{E_b}{N_0 + I_0}\right)_{total} = 10\log_{10}\left(\frac{10^{0.1\times a} \times 10^{0.1\times b}}{10^{0.1\times a} + 10^{0.1\times b}}\right) \ (dB)$$

Alternatively, checking the margin M in the link budget as:

$$SINR = \frac{E_b}{N_0 + I_0}$$

$$SINR = \frac{SNR}{1 + INR}$$

$$\therefore \Delta = 1 + INR \leq M$$

Where, INR is the interference to noise ratio, and Δ is the link degradation caused by the interference.

WFI interfering downlink calculation

As a practical use case, we present in Table II a real design parameter and the link budget computation with interference for the WFI channel.

From these above results, we assumed for our realistic case with INR = 10 dB, which reduces the margin M from 4.9 dB (> minimum required) to −5.55 dB, proving in this punctual case that it is not possible to transmit data using the initial onboard modulator.

We point out that, in the condition of spectrum sharing between FS services and other secondary or co-primary services, the ITU recommends in a relevant publication (ITU 2007), a maximum value for aggregate interference of INR = −10 dB in the X band. This value causes a 'resultant link degradation in margin' Δ = 0.41 dB – maximum specified.

Table II. Link budget results – CBERS-4.

CBERS-4 – WFI FM as-built link budget θ = 62,5°, Plane ϕ = 0°, Freq = 8.29 GHz

MWT ANTENNA		Satellite	Receive Site
E/S LOCATION			**Cuiabá**
LONGITUDE (+)W (-)E	deg		**56,0**
LATITUDE (+)N (-)S	deg		**-17,7**
SATELLITE LOCATION			
HEIGHT	Km	**778**	
TRANSPONDER			
TX EIRP	dBW	**14,5**	
ANTENNA GAIN	dBi	**4,50**	
TX OUTPUT POWER	dBW	**10,0**	
CABLE LOSSES	dB	**0,0**	
MODULATION			
MODULATION		**QPSK**	
INFORMATION RATE	Mbps	**51,28**	
CODE EFFICIENCY	bps/Hz	**1,0**	
SIGNAL BANDWIDTH	MHz	51,28	
PROPAGATION			
DOWNLINK FREQUENCY	MHz	**8290,00**	
CLEAR SKY DOWNLINK LOSS	dB	179,34	
LOSSES			
ATMOSPHERIC / RAIN LOSSES	dB	**1,80**	
EARTH STATION:(E/S)			
RECEIVER G/T	dB/K	**34,5**	
POLARIZATION LOSS	dB	**0,5**	
ANTENNA POINTING LOSS	dB	**0,5**	

Table II. Link budget results – CBERS-4.

CBERS-4 – WFI FM as-built link budget θ = 62,5°, Plane ϕ = 0°, Freq = 8.29 GHz

DOWNLINK BUDGET		
EIRP	dBW	14,5
LOSSES	dB	-182,14
G/T EARTH STATION	dB/K	34,5
BOLTZMANN'S CONSTANT	dBJ/K	228,6
Received C/No (DOWN)	dBHz	95,46
OVERALL LINK BUDGET		
Received C/No (DOWN)	dBHz	95,5
Received Eb/No - loss	dB	15,4
Received Eb/No	dB	18,4
IMPLEMENTATION LOSSES	dB	3,0
DEMODULATION LOSSES	dB	3,0
OTHER LOSSES	dB	0,0
DESIRED Eb/No (BER= 1e-6)	dB	10,5
INITIAL MARGIN	dB	4,9
C/I	dB	8,4
Eb/Io	dB	8,4
Received Eb/(No+Io)	dB	7,95
MARGIN	dB	**-5,55**
INR = I_O/N_O (dB)	dB	10,00
POWER FLUX DENSITY	dBW/m^2 /4kHz	−166, 10

However, in our first approach regarding the ERG operational condition, we assume for the aggregate calculation a value of INR = 10 dB over dimensioning the coexistence model. We will verify in practice that this situation occurs due to the elevated levels of interference received by the station, substantiated by the multiple reflections in the interference environment, the reception by the secondary lobes of the antenna, etc. For *INR* = 10 dB, we have a link degradation Δ = 10.41 dB,

which must be supported for our MODCOD/CR-Paradigm adaptation strategy, presented in the next section.

Application method

In this part of our paper, we suggest our solution by presenting the general idea and the formulate the strategy. In summary, we implemented a combination of CR approach in underlay paradigm and MODCOD techniques (in ACM) to mitigate EOS image reception losses due to interference from Fixed Services (FS) systems.

In this way, we developed steps of calculation in the underlay cognitive paradigm for the technique operability that allows the scenario of coexistence of the EESS downlink with the FS terrestrial links on the same frequencies. We considered the dimensions: i) power *P*; ii) frequency f_c; iii) modulation MOD; iv) coding COD; and v) bandwidth *BW*. The aim is to enable the satellite transmitter with a cognitive function to protect the EESS receiver from the FS interference, by improving the SINR (Signal to Interference plus Noise Ratio) value.

Across the simulations of link budgets for distinct standardized configurations DVB-S2X – MODCOD, we performed the problem-solving strategy applied to spectral coexistence and data throughput maximization adapting the MODCOD functionality. The variation of *m* bits per symbol in the APSK modulations combined with proper code rates produces the bandwidth values as a function of both symbol the rate and the required SINR.

Considering that the specified BER is a function of the SINR for each MODCOD adapted along each satellite pass over the earth station in the presence of interfering signals, the MODCOD selection depends on the INR, which stems directly from the measurement of $E_b/N_0' \equiv Eb/(I_0+N_0)$ performed by the ES receiver.

This adaptive technique is employed on the WFI camera transmission channel of the CBERS-4 satellite, with a bit rate of 51.28 Mbps, following the parameters enumerated in the link budget presented in the previous section. Hence, the established MODCODs and their properties: denominations, identifications (ID), spectral efficiencies, the ratio between E_b/N_0 and E_S/N_0 (energy per symbol to noise ratio), and the modulated carrier effective bandwidth are shown in Table III. For example, based on this Table III, we can assess that for the MODCOD QPSK 3/5 scheme (ID = 8), the E_b/N_0 required for the specified BER (10^{-7}) has a low value of E_b/N_0 = 1.480 dB, which increases the link margin and allows operating with higher INR values. On the other hand, when considering the 32APSK 8/9 scheme (ID = 1), the required E_b/N_0 = 9.258 dB is high and, as a consequence, the INR must be low to allow this operating scheme.

Thus, by combining the link budget computation (Table II) with the MODCODs (Table III), Table IV presents the MODCOD numerical results to be implemented in the ACM mode selected for the real case application that considers the communication system of the WFI camera from the CBERS-4 satellite (EESS / FS coexistence). Regarding that, we kept the same specified link margin constant on 3 dB (Wertz et al. 2011), as previously defined. As a result of this analysis, we obtain the maximum INR (shaded in gray) that each scheme support.

Table III. Adaptive MODCOD in DVB-S2X.

MODCOD	ID	Spectral Efficiency	E_S/N_o (dB) Ideal Frame of 64800 bits	E_b/N_o [dB]	Symbol BW (MHz)
QPSK 1/3	9	0.656448	−1.24	0.587996705	78.12
QPSK 3/5	8	1.188304	2.23	1.48072441	43.15
QPSK 5/6	7	1.654663	5.18	2.992904443	30.99
QPSK 9/10	6	1.788612	6.42	3.894838598	28.67
8PSK 3/4	5	2.228124	7.91	4.430606434	23.01
8PSK 5/6	4	2.478562	9.35	5.40800213	20.69
8PSK 9/10	3	2.679207	10.98	6.699937308	19.14
16APSK 5/6	2	3.300184	11.61	6.424618456	15.54
32APSK 8/9	1	4.397854	15.69	9.257591924	11.66

NOTE: Given the system spectral efficiency η_{tot} the ratio between the energy per information bit and single sided noise power spectral density: $E_b/N_0 = E_s/N_0 - 10log_{10}(\eta_{tot})$.

Table IV. Parameter results from expressions of the link budget calculations subsection.

OVERALL LINK BUDGET		QPSK $\frac{1}{3}$ ID=9	QPSK $\frac{3}{5}$ ID=8	QPSK $\frac{5}{6}$ ID=7	QPSK $\frac{9}{10}$ ID=6	8PSK $\frac{3}{4}$ ID=5	8PSK $\frac{5}{6}$ ID=4	16APSK $\frac{5}{6}$ ID=3	8PSK $\frac{9}{10}$ ID=2	32APSK $\frac{8}{9}$ ID=1
Received C/N_o (Down)	dBHz	95.5	95.5	95.5	95.5	95.5	95.5	95.5	95.5	95.5
Received E_b/N_o- loss	dB	15.4	15.4	15.4	15.4	15.4	15.4	15.4	15.4	15.4
Received E_b/N_o	dB	18.4	18.4	18.4	18.4	18.4	18.4	18.4	18.4	18.4
Implementation Losses	dB	3.0	3.0	3.0	3.0	3.0	3.0	3.0	3.0	3.0
Demodulation Losses	dB	3.0	3.0	3.0	3.0	3.0	3.0	3.0	3.0	3.0
Other Losses	dB	0.0	0.0	0.0	0.0	0.0	0.0	0.0	0.0	0.0
Desired E_b/N_o (BER = 1×10^{-6})	dB	0.6	1.5	3.0	3.7	4.4	5.4	6.4	6.7	9.3
C/I	dB	1.9	5.4	8.4	9.6	11.3	12.8	15.2	14.6	19.9
E_b/I_o	dB	3.9	4.9	6.5	7.6	8.2	9.4	10.7	11.1	15.2
Received $E_b/(N_o+I_o)$	dB	3.58	4.48	5.98	6.91	7.45	8.42	9.43	9.69	12.26
Specified Margin (M)	dB	2.99	3.00	2.99	3.01	3.02	3.02	3.001	2.994	2.998
INR = I_o/N_o (Max Supported)	dB	**14.62**	**13.69**	**12.10**	**11.14**	**10.56**	**9.49**	**8.34**	**8.02**	**4.88**

We relate this result as the first contribution of this article: optimizing downlink performance on the WFI camera transmission channel from CBERS-4, removing the interference effects in the coexisting system scenario (satellite with fixed services). We verify this in Figure S1, based on Table IV results.

Consequently, as the interference power rises, which in turn increases the INR, the system automatically selects the suitable MODCOD to support the current INR value, keeping the bit rate transmission constant.

RESULTS

Case studies of maximum throughput

Throughput for fixed modulation - without interference

Based on the previous results, this section quantifies the throughput for different assumptions. Firstly, we define the baseline case, considered as nominal satellite operations, i.e., the maximum channel rate transmitted in the X band with fixed QPSK modulation without channel coding, as implemented on the CBERS-4 satellite. In this case, the available bandwidth of 51.28 MHz for the WFI camera is limited to 51.28 Mbps. Note that the throughput (T_{hr}) depends on the duration of the satellite pass in visibility with the ERG. By considering an average time of approximately 12 minutes (INPE 2022), we have:

$$T_{hr} = 36.922\ Gbits$$

Which represents the minimum throughput for WFI transmission.

Throughput for fixed modulation - with interference:

By implementing the same fixed QPSK modulation without channel coding in a hypothetical interfering scenario, where the INR changes with the elevation angle of the receiving antenna, we obtain the following results presented in Table V.

It is noteworthy that the throughput is below the minimum for imaging transmission without failures (36.922 Gbits). In this case, we would observe failures in image processing.

$$T_{hr} = 30.988\ Gbits$$

1. Throughput using MODCOD in adapted ACM mode - with interference:

Finally, as the second contribution of this article, we analyze the effectiveness of our proposed strategy on Table VI, by varying the ACM as a function of the INR, in a satellite passage.

Table V. Throughput for QPSK without channel coding, in an interference scenario. (INR X Elevation).

ELEVATION (°)	INR (dB)	% of time[2] (CCSDS 2013)	R_b[1] Mbps	T_{hr}[2] Gbits
90	8.01	16.6	51.28	
75	8.37	13.6	51.28	
60	9.44	25.2	51.28	30.988
30	11.45	35.4	39.65	
5.7	13.70	9.2	6.45	

Notes: [1] The bandwidth is limited of 51.28 MHz;[2] Visibility of 12 minutes (elevation of 0° a 180°).

Table VI. Throughput X MODCOD (in ACM), with interference.

C/I dB	INR dB	ELEVATION (°)	MODCOD ID	% of time[2]	R_b[1] Mbps	T_{hr}[2] Gbits
14.6	8.01	90	8PSK 9/10	16.6	137.39	
15.2	8.37	75	16APSK 5/6	13.6	169.23	
12.8	9.44	60	8PSK 5/6	25.2	127.1	82.878
9.6	11.45	30	QPSK 9/10	35.4	91.92	
5.4	13.70	5.7	QPSK 3/5	9.2	51.28	

Notes: [1] Bandwidth is limited of 51.28 MHz; [2] 12 min.

Thus, we observe that the throughput (82.878 Gbits) is higher than the minimum for WFI imaging transmission (computed as 36.922 Gbits). In this case, we would not expect failures in image processing.

New interference tests in Cuiabá/real scenario – December 2022

Extending the previous results, as the third contribution of this article, we apply our design strategy in an empirical scenario by considering the field measurements recently performed at the Cuiabá (CBA) site in December 2022.

As we previously introduced, the CBA-ERG (station) receives TM signals during the CBERS-4 (C-4) and AMAZONIA-1 (AMZ-1) satellites passing, transmitting the image TM of the satellite payload cameras in real-time.

We perform the interference characterization according to the settled planning: 1) measuring the interfering signal power in the ERG receiver as a function of the azimuth and degrees of antenna elevation; 2) comparing this interference with the desired signal power levels received

from the satellite. In this sense, it is possible to obtain the carrier-to-interference ratio (C/I) and interference-to-noise ratio (INR), which are necessary to perform the proposed strategy. We emphasize at this point that the presence of interferences, considering their operational parameters and spatial distribution (in terms of azimuth X elevation) are time-varying, depending on the SLP operation and technological advances of wireless networks as a function of the larger bandwidth and new mobile services.

To sum up, for our test procedure, we operate with two ERG reception systems: the first one is a higher performance system, comprising an antenna with 11.28 m of diameter; in the second, considered as a spare system, we employ a 10 m antenna. In addition, we connected splitters at the intermediate frequency (IF) points for connecting a high-performance Signal Analyzer at the receiver input, to accurately measure the interference. Figure S2 summarizes the implemented setup.

Next, we represent the azimuthal position for the ERG antennas in Figure S3.

In our first setup, we consider the 11.28 m antenna. The maximum tracked interference that generates failures on the WFI images of the C-4 satellite is present at Az = 333.5° (shown in Table VII). Through further investigation on site, we identified the FS transmitting antenna at the corresponding azimuth, seen in Figure S4.

Table VII presents test results of interference power as a function of the elevation angle of the 11.28 m reception antenna. This reception system assumes a G/T performance of 35.5 dB. Additionally, it is implemented an automatic gain control (AGC) when the reception loop goes into auto-tracking mode, which means that the satellite signal level remains stable (low variation) during the whole satellite visibility.

We emphasize that the AGC also controls the interfering signal level when we monitor the satellite passage in auto-tracking. However, this AGC effect should not be considered when we conduct static interference measurements (as presented in Tables VII and VIII).

Table VII. Interference levels versus elevation of reception antenna at Az (max. interf.) = 333,5° (@ fc = 8308 MHz).

Elevation (°)	*I* (dBm)
0	-33
10	-21
20	-32,5
30	-40,5
40	-47,5
50	-40,5
60	-45
70	-44
77,8	-26,5
80	-39
90	-44
Opposite side (Az=211,9°)[1]	
100	-42
110	-42,5
120	-42,5
130	-41,5
140	-40
150	-37
160	-33,5
170	-34,5
172,63	-32
180	-34

Note [1]: The ERG receiving antenna is positioned and moved from Az = 333.5° to the opposite of the corresponding TX side at Az = 211.9° (i.e., interference in both directions – full-duplex transmission). Due to the geographical position of the antenna, there are no zenith passes on the ERG. For this reason, the measured levels do not correspond to the exact passes of the satellites, but certain orbits will be close to these azimuths.

Complementing the previous measurement, Figure S5 presents the power spectrum of the FS interference signal at the central frequency (f_c) of 8308 MHz @ BW = 37 MHz. It is worth noting that the interference is located in the operational bandwidth of WFI C-4, f_c = 8290 MHz @ BW = 51.28 MHz. Furthermore, we can observe other FS channels interfering in this spectrum window, which can also degrade the WFI processing image.

The harmful interference effect can be observed on the moving-window image of this satellite passage, present in Figure S6.

With all considerations above, we can apply our CR proposed strategy (discussed in the 'application method' subsection) as a function of on-site measured interference. The MODCOD is chosen adaptively during the satellite visibility, varying according to computed INR for different elevation angles of the receiving antenna (Table VIII). Note that we considered the current parameters of the WFI link for C-4.

Table VIII. Calculation of throughput X adaptive MODCOD – C-4 passage.

Elevation (°)	*I* (dBm)	*C* (dBm)	*C*/*I* (dB)	*INR* (dB)[(1)]	MODCOD (ID)	R_b(Mbps)	Time[(2)]%
10	-21	-20,2	0,8	18,97	9 → → *M=-1.05dB*	0	5,88
20	-32,5	-19,7	12,8	6,97	4	121	5,88
30	-40,5	-18,7	21,8	-2,03	1	225,52	5,88
40	-47,5	-18,4	29,1	-9,33	1	225,52	5,88
50	-40,5	-17,9	22,6	-2,83	1	225,52	5,88
60	-45	-16,4	28,6	-8,83	1	225,52	5,88
70	-44	-16,2	27,8	-8,03	1	225,52	5,88
77,8	-26,5	-14,7	11,8	-7,97	5	114,26	5,88
90	-44	-14,1	29,9	-10,13	1	225,52	5,88
100	-42	-14,2	27,8	-8,03	1	225,52	5,88
110	-42,5	-15,2	27,3	-7,53	1	225,52	5,88
120	-42,5	-15,2	27,3	-7,53	1	225,52	5,88
130	-41,5	-16,7	24,8	-5,03	1	225,52	5,88
140	-40	-17,7	22,3	-2,53	1	225,52	5,88
150	-37	-18,2	18,8	0,97	3	169,23	5,88
160	-33,5	-18,7	14,8	4,97	2	137,39	5,88
170	-33	-18,7	14,3	5,47	4	127,10	5,88

[(1)] *BW* = 52 MHz / BW_I = 37 MHz; [(2)] Uniform distribution between 10° and 170°. (Unlike previous analyzes where we considered a distribution specified by CCSDS, in this case, for easiness presentation, we will assume a uniform distribution for our real scenario in question.

T_{hr} = 133.3 *Gbits*

As we can observe, the proper operation of MODCOD transitions mitigates the effects of interference by keeping the margin higher than specified during satellite visibility, except for extremely low elevation angles. Throughput for this configuration is about 3.5 times the minimum required of 36.9 Gbits. In this case, we would not expect failures in image processing.

It is worth mentioning that, considering the reflections and receptions at the antenna's secondary lobes, it has been verified that the interference levels are not decreasing as the elevation angle of the antenna rises. Therefore, in the practical scenarios, we must consider this assumption to increase the accuracy of the results and analyses.

Additionally, we must concentrate on CR awareness in the underlay paradigm through spectral sensing in the surrounding environment, and these interferences sensing is accomplished by monitoring the SINR in the ERG receiver input.

Due to the facts mentioned in the previous paragraph (reflections & second lobes), it is not possible to predict analytically the interference plus noise levels, which reinforces this Cognitive Radio awareness approach combined with the MODCOD technique for our strategy purpose.

Another point to highlight is the link budget parameters in VIII– MODCOD adaptation (*BW* Efficiency X Low Complexity): in our use case, we consider the link closure with a 3 dB margin to get the maximum data throughput, which implies a modulator system of high technical complexity for its development. In considering another approach, we can recalculate the MODCOD to achieve the minimum throughput necessary for WFI data transmission, and in return, we will have a low-complexity technology modulator. This trade-off should be reevaluated regularly, considering the reception systems of the ERG, i.e., a low-cost station might need this last solution. On the other hand, when the reception system is composed by a high-performance receiver with high G/T, we can transmit a much higher data rate, including other recorded passages, since we have higher throughput capacity.

Following the same procedure, we consider our second reception system composed by a 10 m antenna, often used as spare system of the ERG. In this measurement, we receive the WFI of the AMZ-1 satellite (Starting Az = 332.9° / Final Az = 225.5°). Figure S7 presents the power spectrum of the FS interference signal at the central frequency (f_c) of 8308 MHz @ BW = 37 MHz. It is worth noting that the interference is located in the operational bandwidth of WFI AMZ-1, f_c = 8300 MHz @ BW = 51.28 MHz. Furthermore, we can observe other FS channels interfering in this spectrum window, which can also degrade the WFI processing image.

We can highlight the proximity of this geographic coordinate above to the worst-case interference measurements at Az = 320,04° @ f_c = 8308 MHz , designated in Table IX.

Table IX also presents the adaptation strategy of MODCOD for WFI AMZ-1 worst interfering scenario with the computation of the solution parameters.

Table IX. Calculation of throughput X adaptive MODCOD – AMZ-1 passage.

Elevation (°)	P_I (dBm/52 MHz)	P_{signal} (dBm) (max pass)	P_{signal} (dBm/52MHz)	C/I (dB)	INR (dB) (1)	MODCOD (ID)	R_b (Mbps)
5,39	-49	-54	-43,2	5,8	13,97	8	60,94
10	-60	-54	-43,2	16,8	2,97	2	137,39
20	-61	-54	-43,2	17,8	1,97	2	137,39
30	-57,5	-54	-43,2	14,3	5,47	4	127,10
40	-55	-53,5	-42,7	12,3	7,47	5	114,26
50	-58,5	-53,5	-42,7	15,8	3,97	2	137,39
60	-60,5	-53	-42,2	18,3	1,47	3	169,23
70	-63,5	-53	-42,2	21,3	-1,53	1	225,52
80	-70	-52,5	-41,7	28,3	-8,53	1	225,52
90	-70	-52,5	-41,7	28,3	-8,53	1	225,52
100	—	-52,5	-41,7			1	225,52
110	—	-53	-42,2			1	225,52
120	—	-53	-42,2			1	225,52
130	—	-54	-43,2			1	225,52
140	—	-55	-44,2			1	225,52
150	—	-56	-45,2			1	225,52
160	—	-56	-45,2			1	225,52
170	—	-56	-45,2			3	169,23
180	—	-56	-45,2			3	169,23

(1) BW = 52 MHz / BW_I = 37 MHz.

T_{hr} = 131.7 *Gbits*

In the same way as our last result, in which we considered the 11.28 m antenna, the throughput is higher (around 3.5 times) than the minimum required during the satellite visibility. Thus, in this case, we also would not expect failures in image processing.

As in the previous case, this study considers link closure with a 3 dB margin to obtain the maximum BW efficiency; therefore, the comments about the BW Efficiency X Low Complexity trade-off are present.

Regarding the tests, we can consider that the measurements obtained fulfilled the expectations, marking that the interference behavior around the reception antennas has no distributions theoretically predicted due to both reflections in the surrounding environment and the different front-to-back relationships of the antennas. In addition, signals are also received by the secondary lobes of antennas (this shows that the specifications do not remain accurate due to the prolonged period of operation).

DISCUSSION

Tables VIII and IX show the adaptation of the MODCOD necessary to support the INR as a function of the antenna elevation for the azimuthal point of greatest interference, based on calculations performed on the budget of the EOS downlink in the presence of interference. We can conclude that, for the real case of ERG reception at the Cuiabá site, the strategy proposed in this work mitigates the effects of interference in satellite images, except in certain specific points and for specific low elevation angles, which can be retransmitted in another point, since the throughput is more than enough for all coverages.

Referring, therefore, to the throughput of the passages, we find that the value is higher than necessary for the entire transmission of images from the WFI – which requires T_{hr} = *36.922* Gbits, i.e., T_{hr} = *133.3* Gbits for the 11.28 m antenna and T_{hr} = *131.7* Gbits for the 10 m antenna (for maximum bandwidth efficiency). And, as previously highlighted, if it is necessary to operate with less complex systems, the solution can be reevaluated/recalculated for this purpose without WFI image processing failure.

CONCLUSIONS

The main article's purpose was to present a technical solution to allow the coexistence in the same frequency band between fixed terrestrial service links and Earth exploration services by LEO satellites. The solution allows the optimization throughput for high data rates in an interfering environment and maintains the mission BER requirement within the specified value for various levels of interference power spectral density plus noise during the entire passage of the satellite, transmitting the image data telemetry.

We design and develop a technique combining CR exploitation techniques in an underlay paradigm with a reconfiguration of the adaptive MODCOD technique to achieve the target. Therefore, the technique consists of monitoring the SINR per receiving antenna elevation angle for adapting the required MODCOD with the technical goal of receiving data from Earth observation images without errors, fulfilling the required BER during whole satellite-ERG passage visibility.

The application of adaptive MODCOD techniques, based on the DVB-S2X standard, combined with Cognitive Radio approaches that allow expanding the data rate in the specific spectral utilization bandwidth, were used to obtain a higher data transmission rate between the satellite and ground stations.

The results of case studies from C-4 and AMZ-1 link budget calculations of the WFI camera data prove that the MODCOD adaptation technique mitigates the effects of interfering signals present in the ERG of Cuiabá.

REFERENCES

ADDABBO P, ANTONACCHIO F, BELTRAMONTE T, DI BISCEGLIE M, GERACE F, GIANGREGORIO G & ULLO S. 2014. A review of spectrally efficient modulations for earth observation data downlink. In: 2014 IEEE Metrology for Aerospace (MetroAeroSpace), p. 428-432. doi:10.1109/MetroAeroSpace.2014.6865963.

AEB. 2022. PNAE: Programa Nacional de Atividades Espaciais: 2022-2031. URL http://www.gov.br/aeb/pt-br/programa-espacial-brasileiro/politica-organizacoes-programa-e-projetos/programa-nacional-de-atividades-espaciais.

ANATEL. 2013. Regulamentação do serviço limitado privado: resolução nº 617, de 19 de junho de 2013. URL https://informacoes.anatel.gov.br/legislacao/resolucoes/2013/480-resolucao-617.

BOUSQUET M & MARAL G. 2009. Satellite communications systems: systems, techniques and technology. Springer.

CCSDS. 2013. CCSDS space link protocols over ETSI DVB-S2 standard. Standard CCSDS 131.3-B-1. Consultative Committee For Space Data Systems. Washington, D.C., USA.

CCSDS. 2014. radio frequency and modulation systems: recommended standard – Part 1: Earth stations and spacecraft. Standard CCSDS 401.0-B. Consultative Committee For Space Data Systems. Washington, D.C., USA.

CCSDS. 2021. CCSDS space link protocols over ETSI DVB-S2X standard. Standard CCSDS 131.31-O-1. Consultative Committee For Space Data Systems. Washington, D.C., USA.

COLIN T, MILLERIOUX J & DUDAL C. 2016. System Performance of DVB-S2 VCM and ACM High Data Rate Telemetry in EESS Ka-band. SLS-CS_16-09, CCSDS Coding & Synchronization Working Group.

DA SILVA LBC, BENADDI T & FRANCK L. 2020. On the feasibility of a secondary service transmission over an existent satellite infrastructure: design and analysis. EURASIP J Wirel Commun Netw 2020: 1-18.

ETSI. 2016. electromagnetic compatibility and Radio spectrum Matters (ERM) – System Reference document (SRdoc): cognitive radio techniques for satellite communications operating in Ka Band. Standard ETSI TR 103 263 V1.2.1. ETSI. URL http://www.etsi.org/deliver/etsi_tr/103200_103299/103263/01.02.01_60/tr_103263v010201p.pdf.

ETSI. 2020. Digital Video Broadcasting (DVB): second generation framing structure, channel coding and modulation systems for broadcasting, interactive services, news gathering and other broadband satellite applications – Part 2: DVB-S2X extentions (DVB-S2X). Standard ETSI EN 302 307-2 V1.2.1. ETSI. URL http://www.etsi.org/deliver/etsi_tr/103200_103299/103263/01.02.01_60/tr_103263v010201p.pdf.

FEDERAL COMMUNICATIONS COMMISSION ET AL. 2003. Establishment of interference temperature metric to quantify and manage interference and to expand available unlicensed operation in certain fixed mobile and satellite frequency bands. Et Docket 3(289).

GARHWAL A & BHATTACHARYA PP. 2012. A survey on dynamic spectrum access techniques for cognitive radio. arXiv preprint arXiv:12011964 .

IBRAHIM M & GALAL I. 2016. Improved SDR frequency tuning algorithm for frequency hopping systems. Etri Journal 38(3): 455-462.

INPE. 2018. INPE's Image Catalog from the CBERS-4 WFI-L2-DN, DGI-INPE, 2018 URL http://www.dgi.inpe.br/catalogo/explore. Accessed in 30/11/2018.

INPE. 2021. ERG - Cuiabá - MT. URL http://www.dgi.inpe.br/assuntos/recepcao-de-dados/erg-cuiaba.

INPE. 2022. Instituto Nacional de Pesquisas Espaciais. Engenharia de satélites. 2022. URL https://www.gov.br/inpe/pt-br/assuntos/produtos/engenharia-de-satelites. Accessed in 30/01/2023.

ITU. 1997. INTERNATIONAL TELECOMMUNICATION UNION. ITU-R SA.1277-0. RECOMMENDATION.

ITU. 2007. Maximum allowable error performance and availability degradations to digital fixed wireless systems arising from radio interference from emissions and radiations from other sources. INTERNATIONAL TELECOMMUNICATION UNION. ITU-R F.1094-2. RECOMMENDATION.

ITU-R. 2016. REGULATIONS, ITU Radio. Frequency allocations. Volume I. URL https://www.itu.int/pub/R-REG-RR-2016/en. Acessed in: 24 September 2020.

MITOLA JI. 2000. Cognitive radio: an integrated agent architecture for software defined radio. Ph.D. thesis. KTH Royal Inst. Technology. Ph. D. Thesis.

SHARMA S. 2014. Interweave/underlay cognitive radio techniques and applications in satellite communication systems. Ph.D. thesis. University of Luxembourg, Luxembourg.

SHARMA S, BOGALE T, CHATZINOTAS S, OTTERSTEN B, LE L & WANG X. 2015. Cognitive radio techniques under practical imperfections: A survey. IEEE Communications Surveys & Tutorials 17(4): 1858-1884.

SHARMA S, CHATZINOTAS S & OTTERSTEN B. 2013. Cognitive radio techniques for satellite communication systems. In: 2013 IEEE 78th vehicular technology conference (VTC Fall). p. 1-5. IEEE.

WANG C, BIAN D, ZHANG G, CHENG J & LI Y. 2018. A novel dynamic spectrum-sharing method for integrated wireless multimedia sensors and cognitive satellite networks. Sensors 18(11): 3904.

WERTZ J, EVERETT D & PUSCHELL J. 2011. Space mission engineering: the new SMAD. (No Title) .

SUPPLEMENTARY MATERIAL

Figures S1-S7.

How to cite

ARAUJO RAS, SILVA LBC, SANTOS WA & SOUZA MLO. 2024. Mitigating interferences on LEO satellite downlinks of Earth exploration services by cognitive radio, adaptive modulation and coding techniques. An Acad Bras Cienc 96: e20230487. DOI 10.1590/0001-3765202420230487.

Manuscript received on May 2, 2023;
accepted for publication on February 4, 2024

RODOLFO ANTONIO DA SILVA ARAUJO[1]
https://orcid.org/0009-0001-2851-3890

LUCIANO B.C. DA SILVA[1]
https://orcid.org/0000-0003-3521-4036

WALTER ABRAHÃO DOS SANTOS[2]
https://orcid.org/0000-0002-6516-6488

MARCELO L. DE OLIVEIRA E SOUZA[3]
https://orcid.org/0000-0003-1309-3333

[1]Instituto Nacional de Pesquisas Espaciais, Divisão de Eletrônica Espacial e Computação - CGCE, Av. dos Astronautas, 1758, 12227-010 São José dos Campos, SP, Brazil
[2]Instituto Nacional de Pesquisas Espaciais, Divisão de Pequenos Satélites - CGCE, Av. dos Astronautas, 1758, 12227-010 São José dos Campos, SP, Brazil
[3]Instituto Nacional de Pesquisas Espaciais, Curso de Engenharia e Tecnologia Espaciais - ETE, Av. dos Astronautas, 1758, 12227-010 São José dos Campos, SP, Brazil

Correspondence to: **Rodolfo Antonio da Silva Araujo**
E-mail: rodolfo.araujo@inpe.br

Author contributions

Rodolfo A. S. Araujo: Conceptualization, Methodology, Design, Software, Data collection, Original draft preparation, Investigation, Analysis, Interpretation and Validation of results, Writing- Reviewing and Editing; Luciano B. C. Da Silva: Conceptualization, Investigation, Supervision, Analysis, Interpretation and Validation of results, Writing- Reviewing and Editing; Walter A. Santos and Marcelo L. O. Souza: Investigation, Supervision, Analysis, interpretation and Validation of results, Writing- Reviewing and Editing.